NASTRAN STRUCTURAL MODEL FOR THE LARGE GROUND ANTENNA PEDESTAL WITH APPLICTIONS TO HYDROSTATIC BEARING OIL FILM

CHIAN T. CHIAN

Jet Propulsion Laboratory, Pasadena, CA

SUMMARY

Investigations were conducted on the 64-meter antenna hydrostatic bearing oil film thickness under a variety of loads and elastic moduli. These parametric studies used a NASTRAN pedestal strutural model to determine the deflections under the hydrostatic bearing pad. The deflections formed the input for a computer program to determine the hydrostatic bearing oil film thickness. For the future 64-meter to 70-meter antenna extension and for the 2.2-meter (86-in.) haunch concrete replacement cases, the program predicted safe oil film thickness (greater than 0.13 mm (0.005 in.) at the corners of the pad). The effects of varying moduli of elasticity for different sections of the pedestal and the film height under distressed runner conditions were also studied.

INTRODUCTION

The upgrade of the large NASA Deep Space Network (DSN) antennas provide the necessary increase in earth-based space communication capability at the following three Deep Space Communication Complexes: Goldstone, California; Canberra, Australia; and Madrid, Spain. (Fig. 1)

The physical diameter of the three large antennas are extended from the existing 64 meters to 70 meters. (Fig. 2) The increase of the antenna aperture and the associated structural and mechanical modifications are needed in support of the Voyager 2 - Neptune encounter in August 1989 (Fig. 3), the Galileo-Jupiter mission (Fig. 4), and ongoing spacecraft communications in our solar system. Radio Astronomy and Search for Extraterrestrial Intelligence (SETI) scientific projects will also benefit from the enchancement.

The pedestal of the large antenna is a two-story, reinforced concrete building, which supports the movable structure of the antenna. (Fig. 5) The pedestal is under pressure loadings at the three hydrostatic bearing pads. A minimum hydrostatic bearing oil film of 0.13 mm (0.005 in.) is required to avoid any metal to metal contact between the pad and the runner and to accommodate any runner malfunctioning and placement tolerance.

This article reports on the static analysis and computer modeling for the large 64-meter antenna pedestal. NASTRAN Program was used to develop the pedestal structural model. The top surface deflection of the pedestal obtained from the NASTRAN model was used as an input to a separate computer program to determine the minimum oil film thickness between the hydrostatic bearing pad and the runner. The knowledge of the oil film thickness was necessary to conduct a variety of hydrostatic bearing rehabilition studies.

Three parametric studies were conducted to evaluate the performance of the hydrostatic bearing system. Effects on the oil film thickness due to the following factors were considered in each of the three parametric studies:

(1) The height of the new concrete in the pedestal haunch area.

(2) The different moduli of elasticity of the concrete in the pedestal wall and haunch area.

(3) The hydrostatic bearing pad load increase due to the planned antenna aperture extension from 64 meters to 70 meters.

The results of these parametric studies are presented in this report.

PEDESTAL DESCRIPTION

The azimuth hydrostatic bearing, set on the pedestal top, supports the full weight of the moving parts of the antenna and permits a very low friction azimuth rotation on a pressurized oil film. (Ref. 1) A cross-sectional diagram of the hydrostatic bearing is shown in Fig. 6.

Three movable pad-and-socket assemblies float on the oil film over a stationary runner and support the three corners of the alidade base triangle as shown in Fig. 7. The stationary runner for the bearing and the three bearing pads are completely enclosed in an oil reservoir. The three hydrostatic bearing pads are equidistant from the central axis of the pedestal as shown in Fig. 8.

The pedestal is 13.7 m (45 ft) tall, 25.3 m (83 ft) in diameter, with a diaphragm top which has a concrete collar in the center; the pedestal supports the movable structure of the antenna. The wall thickness is 1.1 m (3.5 ft).

The three principal forces from the antenna alidade which act on the pedestal are: (1) vertical forces from the azimuth hydrostatic bearing pads, (2) rotational forces from te azimuth drives, and (3) horizontal forces on the azimuth radial bearing.

The three hydrostatic bearing pads, made of carbon steel are 1.Ø16 m (4Ø in.) wide, 1.524 m (6Ø in.) long, and Ø.5Ø8 m (2Ø in.) deep. There are six recesses in the bottom of each pad as indicated in Fig. 9 with the two center recesses being larger than the corner recesses. According to the original design specification, the pedestal concrete is required to have a Young's modulus of elasticity E of $3.5 \times 1Ø^{10}$ N/m^2 ($5.Ø \times 1Ø^{6}$ psi). However, it is believed that the current Young's modulus of elasticity for the pedestal concrete is less than this value, and a reduced value, consistent with current core-sample measurements, is assumed for this report.

DESCRIPTION OF THE NASTRAN MODEL

All three pads are assumed to support the same amount of loads. Therefore, the pedestal is divided into three identical segments. Moreover, due to the symmetry with respect to the center line of the pad, each segment can be further divided into two segments.

As a consequence, a one-sixth segment of the pedestal, with angular span of 60°, is being developed in the present structural model as shown in Fig. 10. Appropriate boundary conditions are being applied to reflect the aforementioned symmetry: (1) zero slope at the points representing the centerline of the pad, and (2) zero slope at the ponts representing midposition between two pads.

The pedestal model is first considered as a cylinder of uniform wall thickness which comprises 630 six-sided solid elements (CHEXA2) with a total of 880 grid points. The actual haunch contour and the top slab is added in the pedestal model to provide additional stiffness on the pedestal wall.

The pedestal concrete is assumed to be homogeneous, with a reduced Young's modulus of elasticity E of 2.8×10^{10} N/m^2 (4.0×10^6 psi). The actual pressure profile of the oil under the hydrostatic bearing pad is exerted on the top pedestal surface (Fig. 11).

For simplicity, the pressure pattern of the oil under the pad is assumed to be symmetric with respect to the pad centerline in the NASTRAN pedestal model. Therefore, $p_1 = p_3$ and $p_4 = p_6$. Pad 3, which experiences the highest load among the three pads, is the one considered in our model. The values of the pad recess pressures are given in Table 1.

DESIGN CHARACTERISTICS

Two design characteristics are used to evaluate the sensitivity of the hydrostatic bearing pad operation to the modulus of elasticity. The first characteristic is the maximum pad out-of-flatness. Deflected shapes of the hydrostatic bearing pad and runner surface are illustrated in Fig. 12. Relative deflections within the hydrostatic bearing pad and within the runner surface (from centerline to edge of pad) are shown as Δ_p and Δ_r, respectively.

Design criteria (Ref. 1) require that the mismatch of deflected surfaces, $\Delta\delta$, be within 0.101 mm (0.004 in.). (This is the variation of the film height between the pad and the runner.) Out of this a maximum mismatch of deflected shapes of 0.076 mm (0.003 in.) was established as the allowance for creep during construction before the bearing pads could be moved. The remaining 0.025 mm (0.001 in.) was the design criteria for mismatch of elastic deformations. Since creep strains have been compensated for by releveling of the runner, the maximuum pad out-of-flatness, a $\Delta\delta$ of 0.101 mm (0.004 in.), can now all be accounted for by elastic deformations. These elastic deformations are part of the NASTRAN output.

The second characteristic used to evaluate the operability of the hydrostatic bearing is the minimum oil film thickness between the pad and the runner. Based on previous operational experience, a minimum oil film thickness, h, of 0.127 mm (0.005 in.) is considered necessary for safe operation. Figure 13 shows

a typical deflection map of the top pedestal surface under pad load. This deflection map is used as the input to the oil film height model to determine the minimum oil film thickness between the pad and the runner.

COMPARISON WITH FIELD MEASUREMENTS

The field measurements were conducted at the Goldstone, California (DSS-14) 64-meter antenna pedestal, and the load-deformation relationships of the pedestal were obtained.

Fig. 14(a) shows the locations of the gauges for deflection measurements. Instruments were installed to measure vertical deformations over a 1.27 m (50 in.) gauge length on the external surface of the haunch and the wall. Figure 14(b) is a schematic of the instrumentation used. As shown, small blocks were bonded to the structure at the preselected locations. A direct current differential transformer (DCDT) mounted in a fixture was attached to the upper block. A wire from the spring-loaded plunger of the DCDT was attached to the lower block. The output of the DCDT was continuously recorded during the time required for antenna Pad 3 to be moved across the instrumented location. This time is approximately 3 minutes.

Figures 15 and 16 show the good correlation between the field deflection measurements and the NASTRAN predicted values for two different locations: azimuth 49° and aximuth 96°.

PARAMETRIC STUDIES

Three parametric studies were conducted to evaluate the operability of the large 64-meter antenna:

(1) Effect on the oil film thickness due to the height variation of the new concrete in the pedestal haunch.

(2) Effect on the oil film thickness due to the variation of concrete elastic moduli in the pedestal wall and haunch area.

(3) Effect on the oil film thickness due to the pad load increase for an antenna aperture extension from 64 meters to 70 meters.

A. Height of New Concrete in the Pedestal Haunch

The pedestal concrete with an initial modulus of elasticity E of 2.1×10^{10} N/m^2 (3×10^6 psi) was replaced by a new concrete with the modulus of elasticity of 3.5×10^{10} N/m^2 (5×10^6 psi) at different heights from the top. Results of this parametric study are shown in Table 2 as well as in Fig. 17.

B. Variation of Concrete Elastic Moduli in the Pedestal Wall and Haunch Area:

The severity of the concrete deterioration with accompanying reduction in compressive strength and modulus of elasticity varies widely throughout the pedestal mass. Studies to date have shown that the most serious damage was in the haunch area. A height of 2.2 m (86 in.) of the concrete in the haunch area has been replaced as part of the rehabilitation efforts.

Portions of the remainng pedestal concrete not replaced have experienced moderate damage and are expected to drop further in strength and modulus of elasticity in the future since the alkali-aggregate reaction (the main reason of deteriorations) is continuous, and not fully understood. Therefore, this study was made to evaluate the operability of the hydrostatic bearing under these continuous deteriorations. The moduli of elasticity of the concrete in the pedestal wall and the haunch area were varied. This study was further subdivided into two parts:

(1) The new haunch area down to a depth 2.2 m (86 in.) was assigned a fixed modulus of elasticity of 3.5×10^{10} N/m^2 (5×10^6 psi), while the modulus of elastic ity of the remaining wall was taken to be 2.1×10^{10} N/m^2 (3×10^6 psi), 1.4×10^{10} N/m^2 (2×10^6 psi), and 0.7×10^{10} N/m^2 (1×10^6 psi), to simulate time deteriorations. Note that tests made on replaced concrete showed E larger than 3.5×10^{10} N/m^2 (5×10^6 psi).

(2) The pedestal wall was assumed to have a fixed modulus of elasticity of 1.4×10^{10} N/m^2 (2×10^6 psi), while the new haunch area was assigned a modulus of elasticity of 3.5×10^{10} N/m^2 (5×10^6 psi), 3.15×10^{10} N/m^2 (4.5×10^6 psi) and 2.8×10^{10} N/m^2 (4×10^6 psi) to simulate different values of the replaced concrete.

Results of this parametric study showing the effect on the oil film thickness due to the variation of concrete elastic moduli are summarized in Tables 3 and 4. Figures 18 and 19 also give the results of this study.

C. Pad Load Increase With an Antenna Aperture Extension From 64 meters to 70 meters

This study investigates the effects of the increased pad load of the antenna with an aperture extension from 64 meters to 70 meters on the pedestal deflection and the oil film thickness. Pad 3 was assumed to have a load of 1.1×10^6 kg (2.4×10^6 lb). In this study, four loads of 1.1×10^6 kg (2.4×10^6 lb.), 1.3×10^6 kg (2.8×10^6 lb), 1.45×10^6 kg (3.2×10^6 lb), and 1.6×10^6 kg (3.6×10^6 lb) were considered for pad 3, which correspond to load factors of 1.00; 1.17; 1.33; and 1.50, respectively, relative to the estimated original 64-meter pad 3 load. The modulus of elasticity was assumed to be 3.5×10^{10} N/m^2 (5×10^6 psi) for both the pedestal wall and the haunch area. The maximum film height variation, $\Delta\delta$, and the minimum film thickness, h, are given in Table 5 for the four loads considered. The results are also shown in Fig. 20.

CONCLUSIONS

In this study we reported on applications of the NASTRAN pedestal model to the hydrostatic bearing oil film for the large 64-meter antenna. The NASTRAN model gave as one result the top surface deflections of the pedestal. These deflections formed the input for the hydrostatic bearing oil film computer program to determine the minimum oil film thickness.

The knowledge of the minimum oil film thickness between the hydrostatic bearing pad and the runner was required to conduct a variety of hydrostatic bearing rehabilitation studies.

Based on results presented in this study, a height of 2.2 meters (86 in.) of concrete in the top-most pedestal haunch area has been replaced in the DSS 14, located in Goldstone, California, as part of the rehabilitation efforts. For a new concrete with the modulus of elasticity of 3.5×10^{10} N/m^2 (5×10^6 psi), the study predicted a safe oil film thickness of more than 0.13 mm (0.005 in.).

The effect on the oil film thickness due to the pad load increase for an antenna aperture extension from 64 meters to 70 meters was also investigated. For a pad load increase of up to 20%, the study predicted a safe oil film thickness.

REFERECE

1. TDA Technical Staff, "The NASA/JPL 64-Meter-Diameter Antenna at Goldstone, California: Project Report", JPL Technical Memorandum 33-671, Jet Propulsion Laboratory, Pasadena, CA, July 15, 1974.

Table 1. Pad 3 Recess Presures[a]

Recess presure	p_1	p_2	p_4	p_5
N/m^2	11,383,000	7,757,000	10,859,000	9,480,0000
psi	1651	1125	1575	1375

[a] Assume $p_1 = p_3 = \frac{1}{2}(p_1 + p_3)$ and $p_4 = p_6 = \frac{1}{2}(p_4 + p_6)$.

Table 2. Effect on the oil film thickness due to the height variation of the new concrete in the pedestal haunch.

Description, N/m^2 (psi)	Film height variation $\Delta\delta$, mm (in.)	Minimum oil film thickness h, mm (in.)
Entire pedestal: $E = 2.1 \times 10^{10}$	0.147	0.132
(3×10^6)	(0.0058)	(0.0052)
Top 1.4 m (56 in.): $E = 3.5 \times 10^{10}$	0.102	0.196
(5×10^6)	(0.0040)	(0.0077)
Remaining pedestal: $E = 2.1 \times 10^{10}$		
(3×10^6)		
Top 2.2 m (86. in.): $E = 3.5 \times 10^{10}$	0.097	0.191
(5×10^6)	(0.0038)	(0.0075)
Remaining pedestal: $E = 2.1 \times 10^{10}$		
(3×10^6)		

Table 3. Effect of varying the modulus of elasticity of the pedestal wall[a]

Modulus of elasticity of the pedestal wall, N/m^2 (psi)	Film height variation $\Delta\delta$, mm (in.)	Minimum oil film thickness h, mm (in.)
2.1×10^{10} (3×10^{6})	0.097	0.193
	(0.0038)	(0.0076)
1.4×10^{10} (2×10^{6})	0.102	0.191
	(0.0040)	(0.0075)
0.7×10^{10} (1×10^{6})	0.119	0.178
	(0.0047)	(0.0070)

a The modulus of elasticity of the top 2.2 m (86 in.) in the haunch is considered to be fixed at 3.5×10^{10} N/m^2 (5×10^{6} psi).

Table 4. Effect of varying the modulus of elasticity of the haunch area[a]

Modulus of elasticity of the top 2.2 m (86 in.) in the haunch, N/m^2 (psi)	Film height variation $\Delta\delta$, mm (in.)	Minimum oil film thickness h, mm (in.)
3.5×10^{10} (5×10^6)	0.102	0.191
	(0.0040)	(0.0075)
3.15×10^{10} (4.5×10^6)	0.112	0.152
	(0.0044)	(0.0060)
2.8×10^{10} (4×10^6)	0.125	0.152
	(0.0049)	(0.0060)

[a] The modulus of elasticity of the pedestal wall is assumed to be fixed at 1.4×10^{10} N/m^2 (2×10^6 psi).

Table 5. Effect of the pad load increase due to the antenna extension[a]

Pad (No. 3) load, kg (lb)	Load Factor	Film height variation, $\Delta\delta$, mm (in.)	Minimum oil film thickness, h, mm (in.)
1.09×10^6	1.00	0.089	0.185
(2.4×10^6)		(0.0035)	(0.0073)
1.27×10^6	1.17	0.104	0.152
(2.8×10^6)		(0.0041)	(0.0060)
1.45×10^6	1.33	0.119	0.122
(3.2×10^6)		(0.0047)	(0.0048)
1.63×10^6	1.50	0.135	0.086
(3.6×10^6)		(0.0053)	(0.0034)

[a] The entire pedestal is assumed to have a modulus of elasticity of 3.5×10^{10} N/m^2 (5×10^6 psi) in all cases.

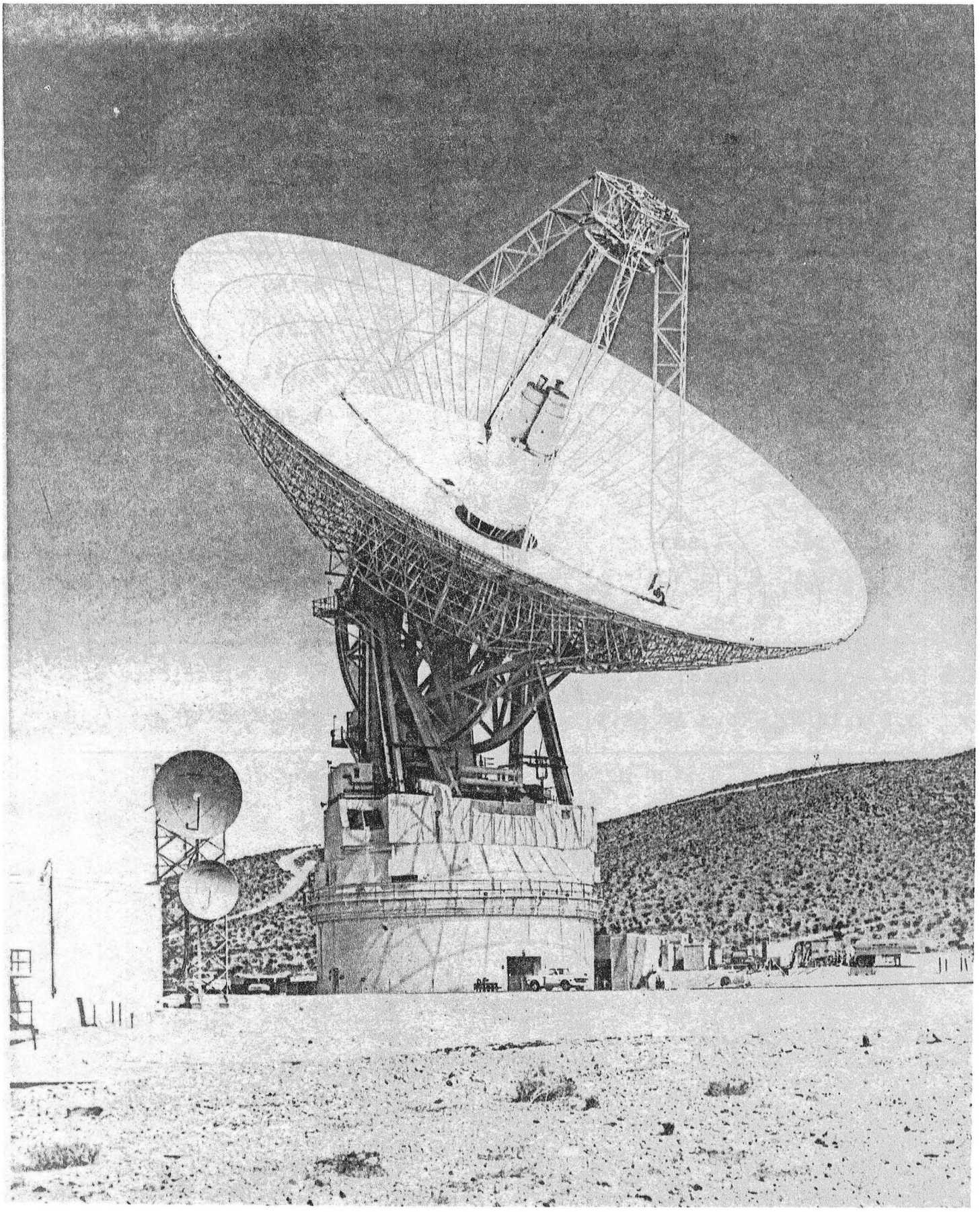

Fig. 1. Large 64-meter NASA Deep Space Network Antenna

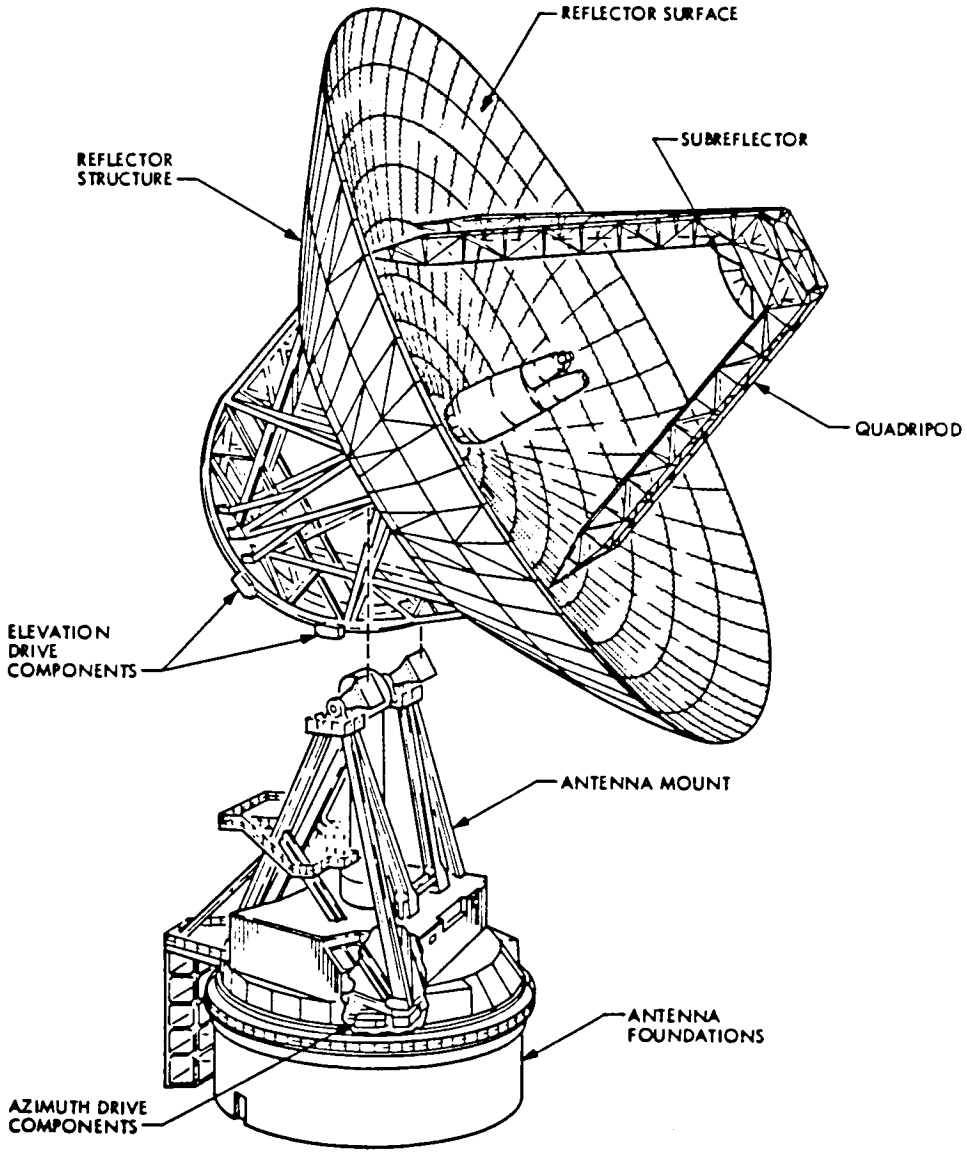

Fig. 2. Antenna Aperture Extension from 64 meters to 70 meters

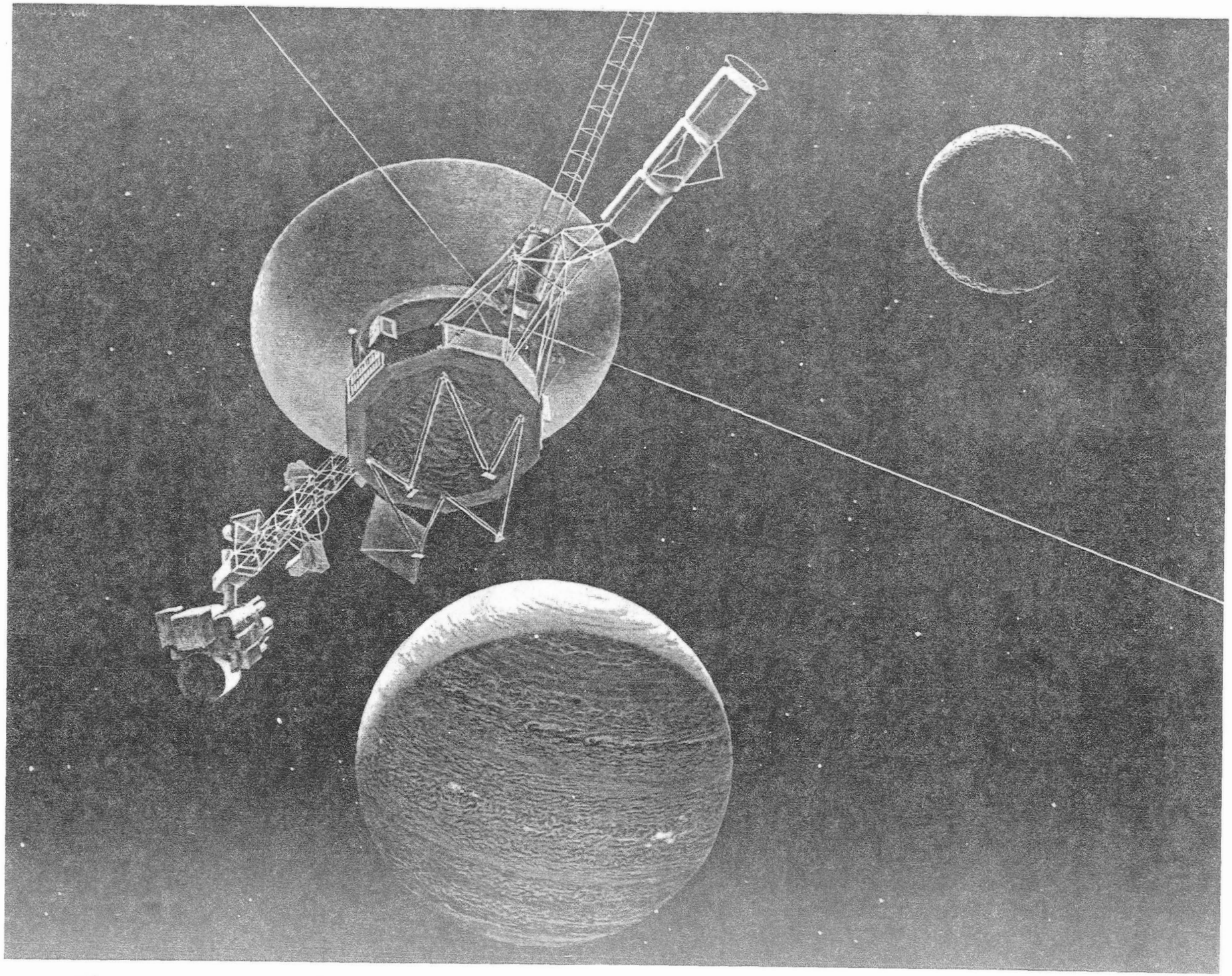

Fig. 3. Voyager 2 makes its closest Encounter with Neptune on August 24, 1989.

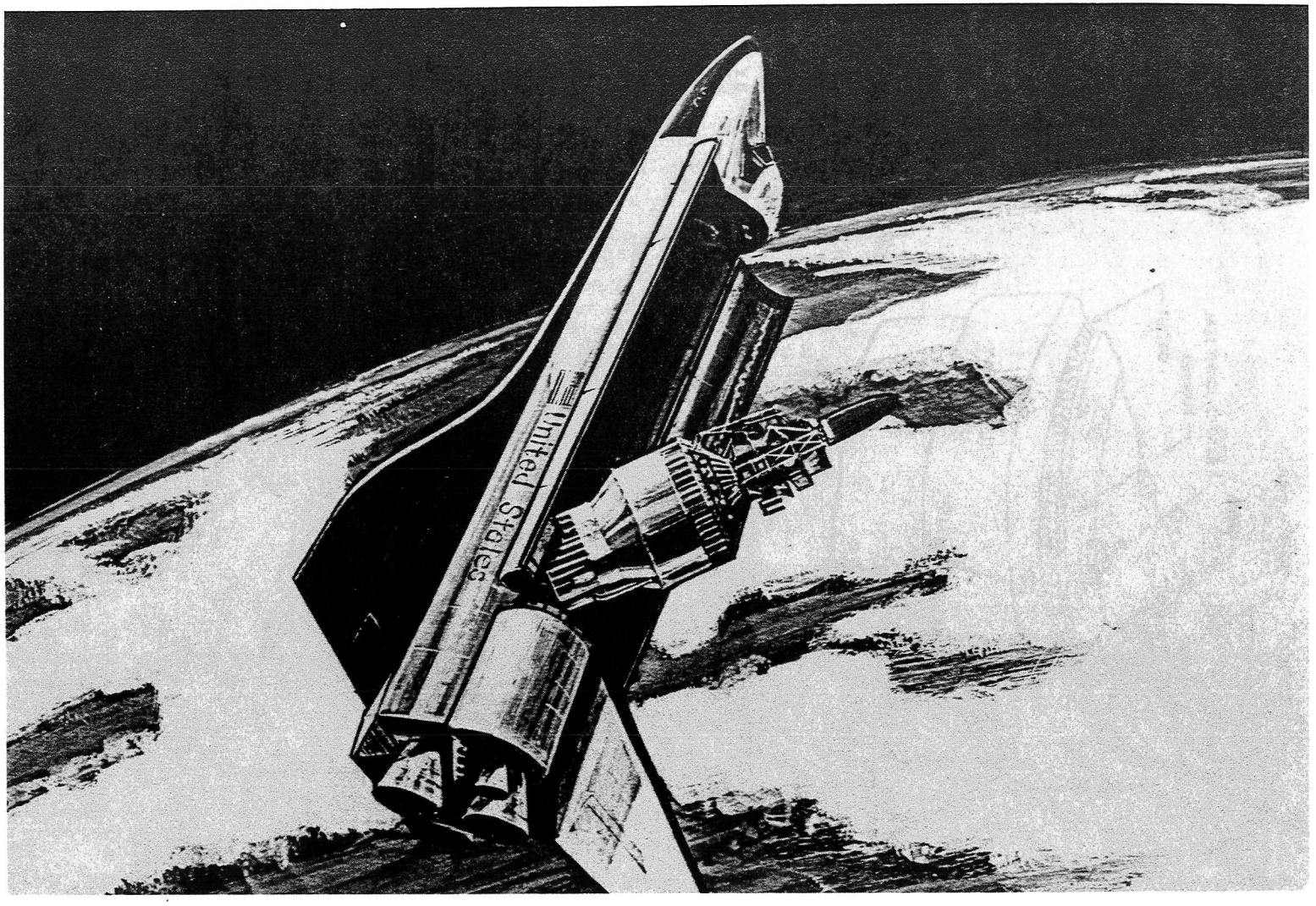

Fig. 4. Galileo Spacecraft to Jupiter is being launched from the space shuttle.

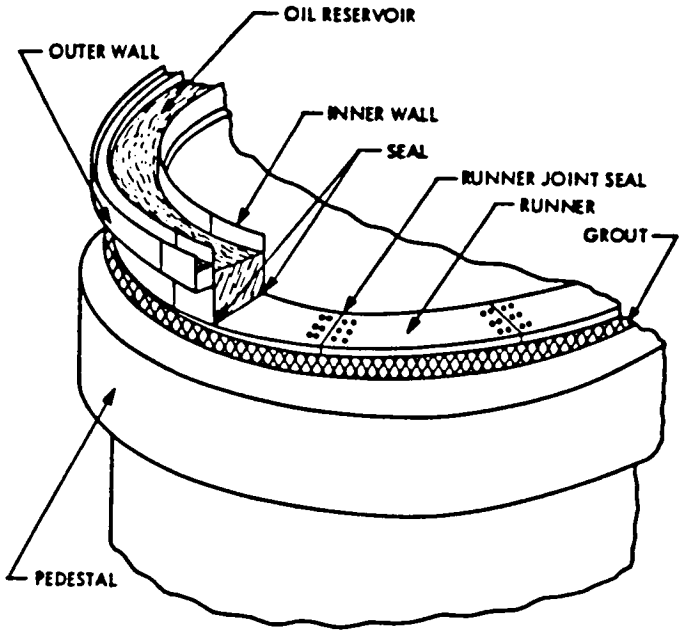

Fig. 5. General arrangement of 64-m antenna hydrostatic bearing

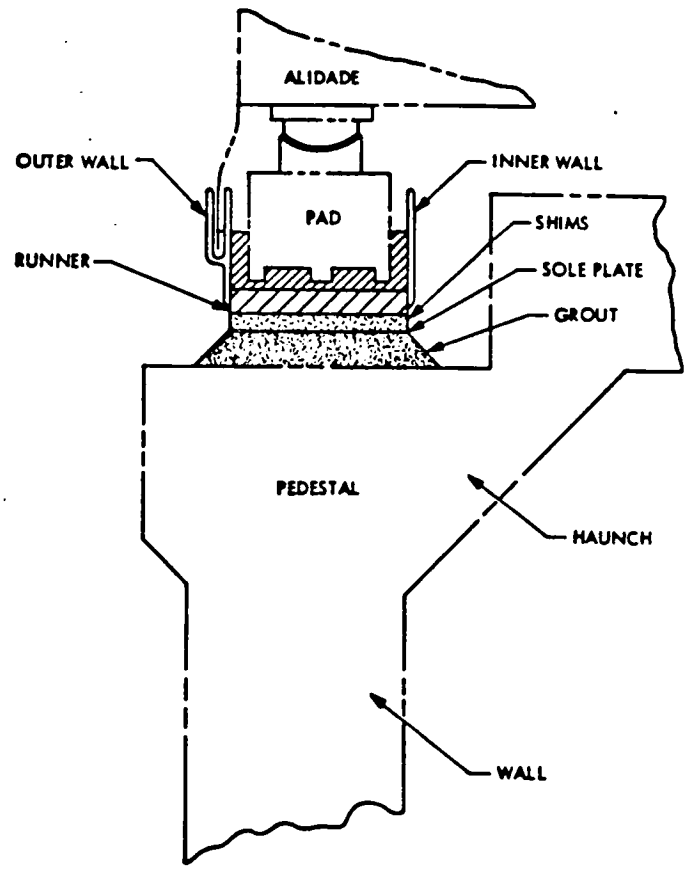

Fig. 6. Cross section of hydrostatic bearing system

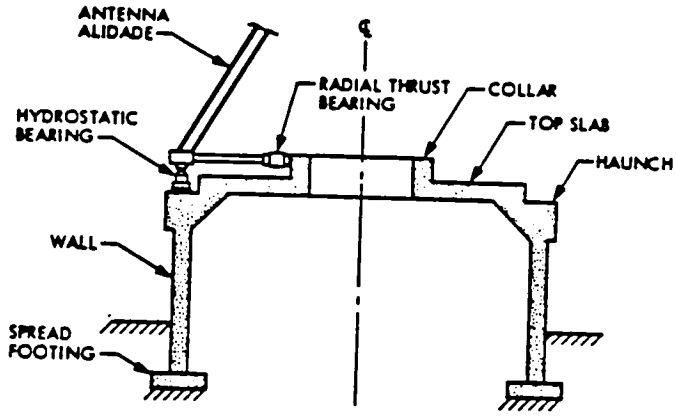

Fig. 7. Cross Section of Concrete Pedestal

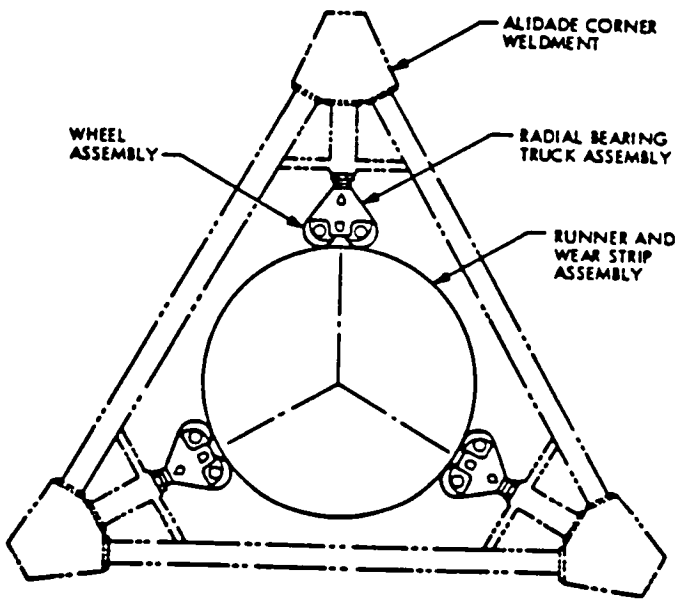

Fig. 8. Alidade base triangle and radial bearing assembly

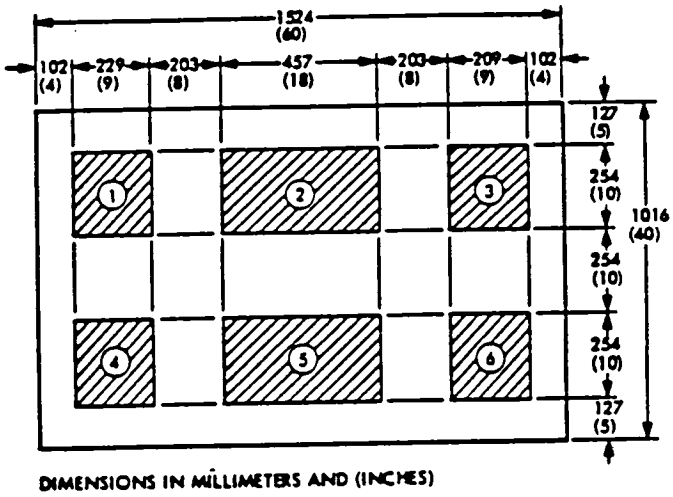

Fig. 9. Recess pattern of hydrostatic bearing pad

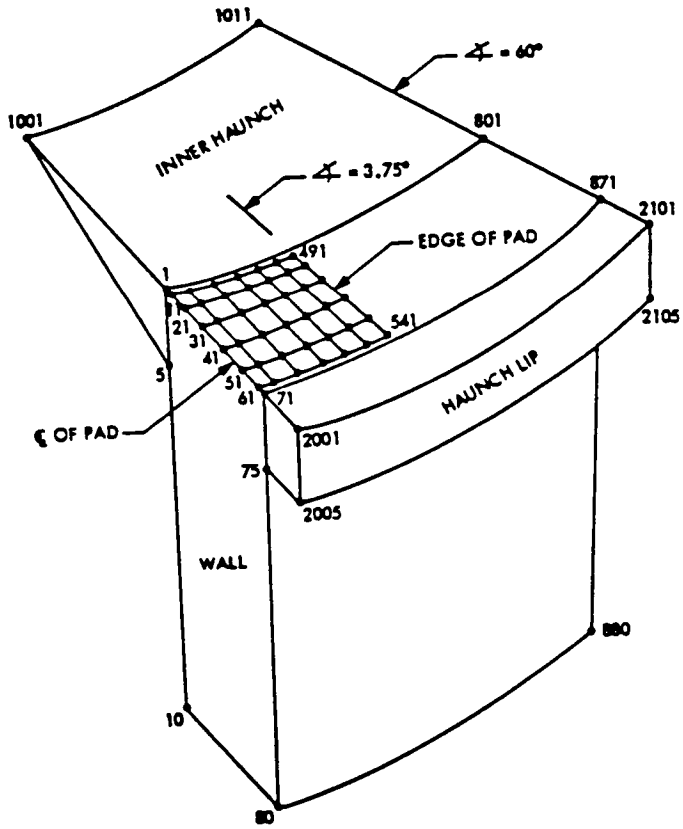

Fig. 10. NASTRAN pedestal model and nodal points

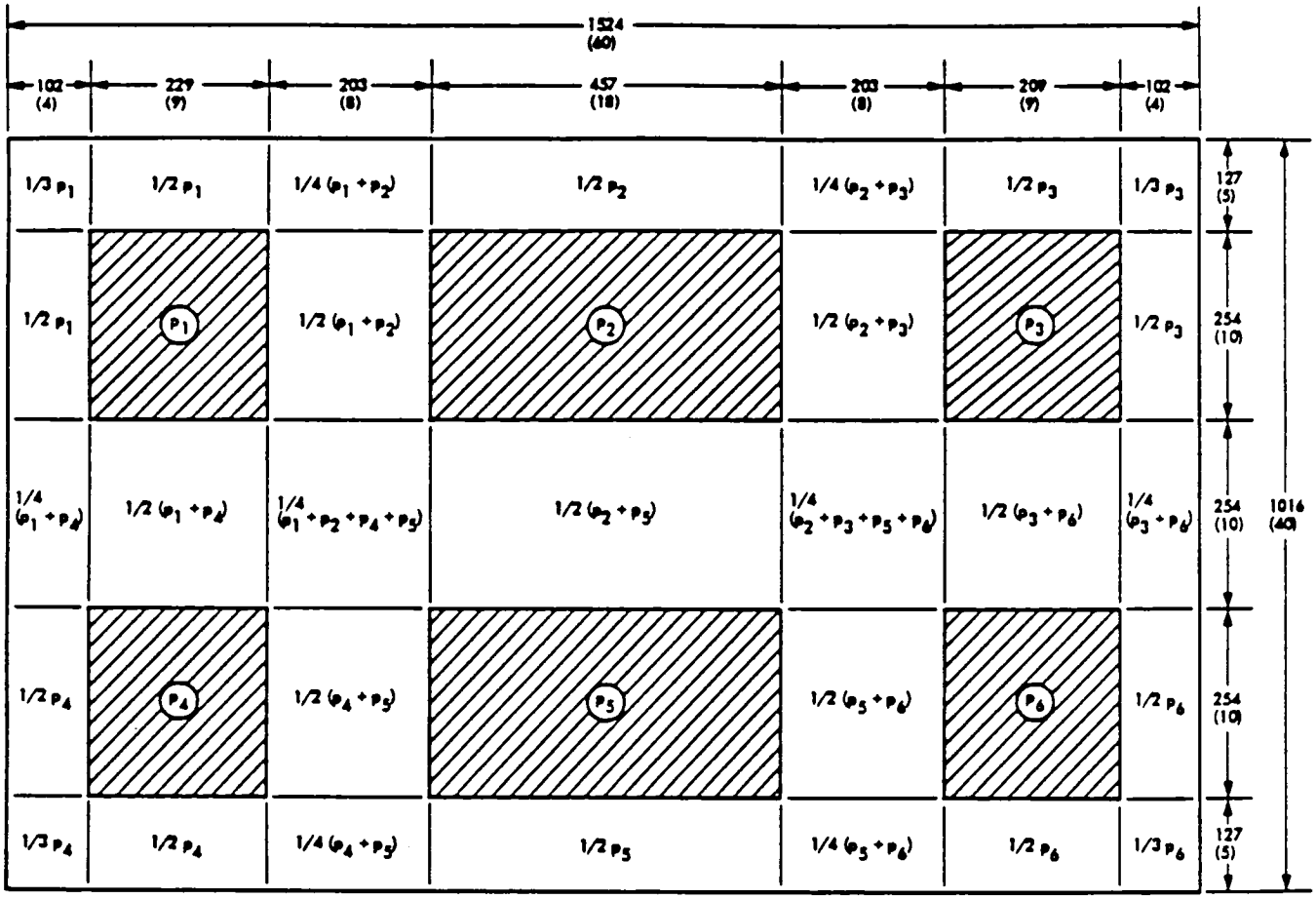

Fig. 11. Pressure profile of hydrostatic bearing pad

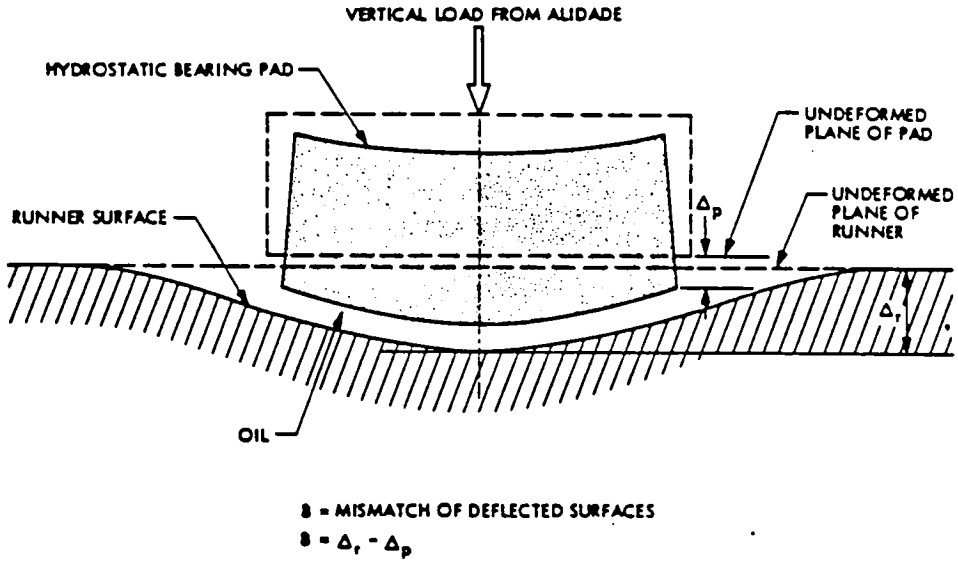

Fig. 12. Deflections of hydrostatic bearing pad and runner surface

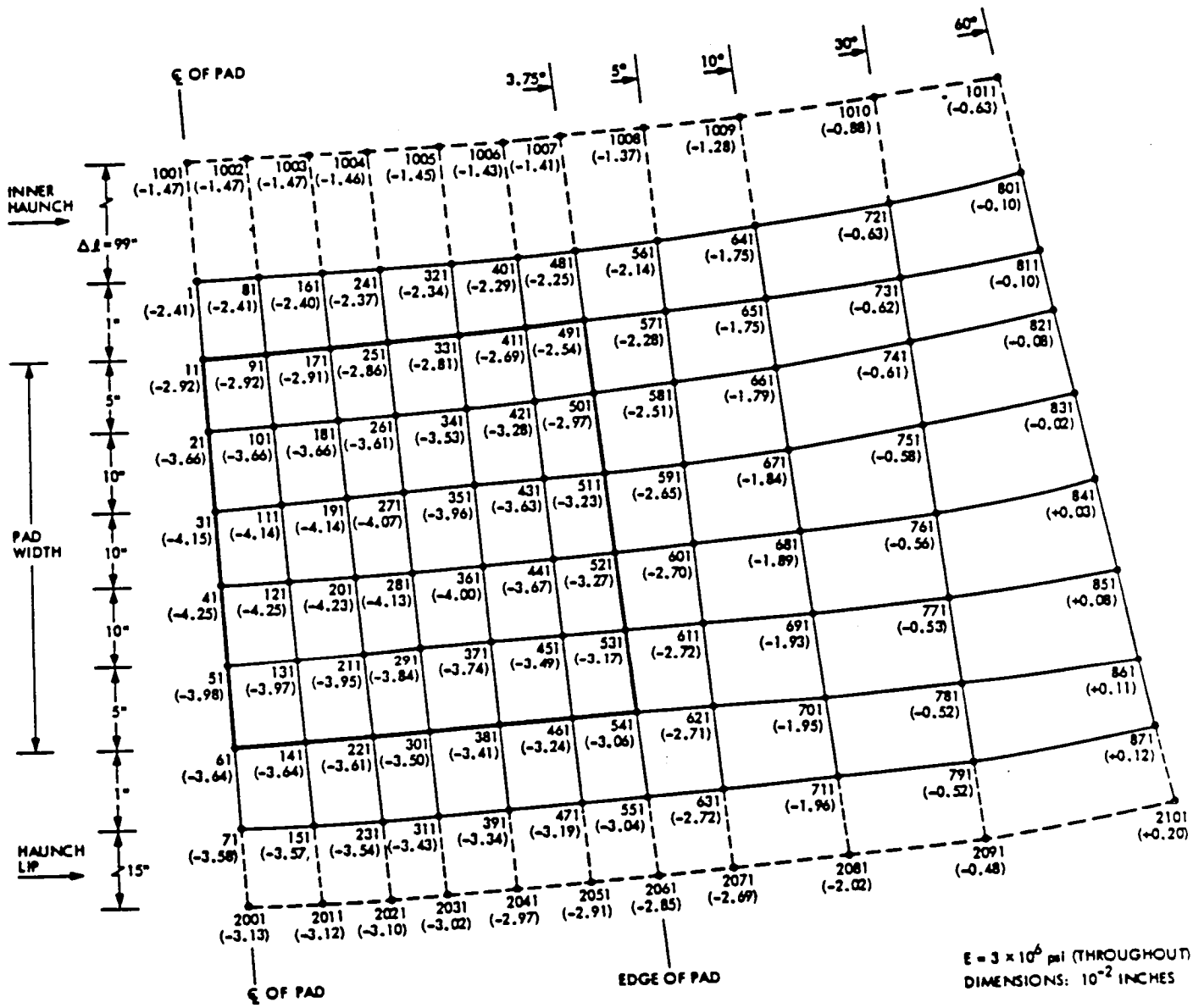

Fig. 13. Deflection map of the pedestal surface

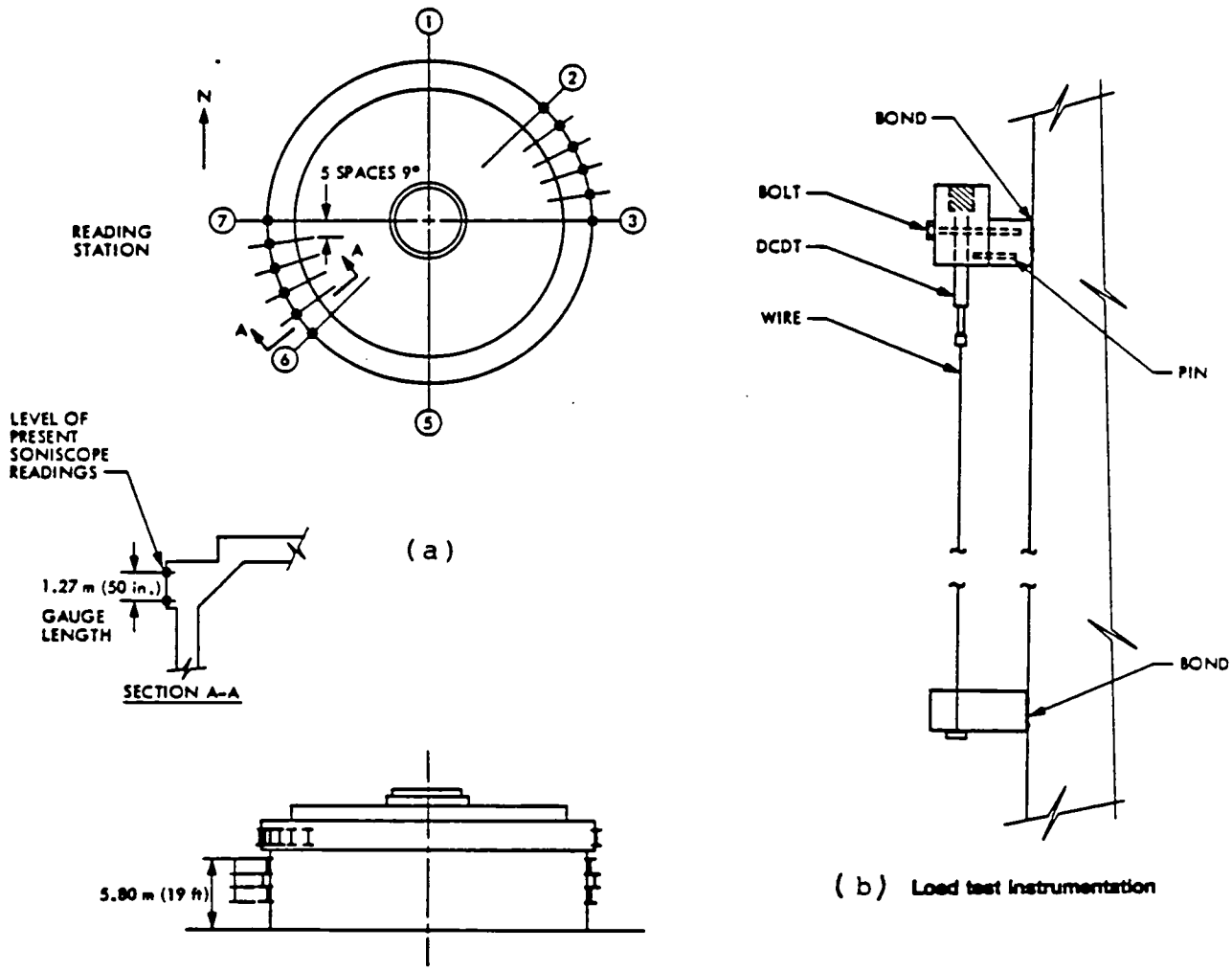

Fig. 14 Location of pad load tests

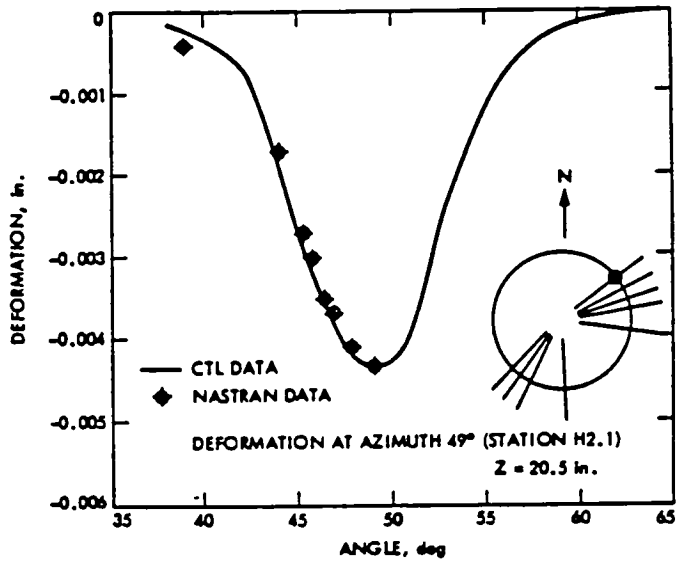

Fig. 15. Comparison of the NASTRAN mode results with field test data, azimuth = 49°

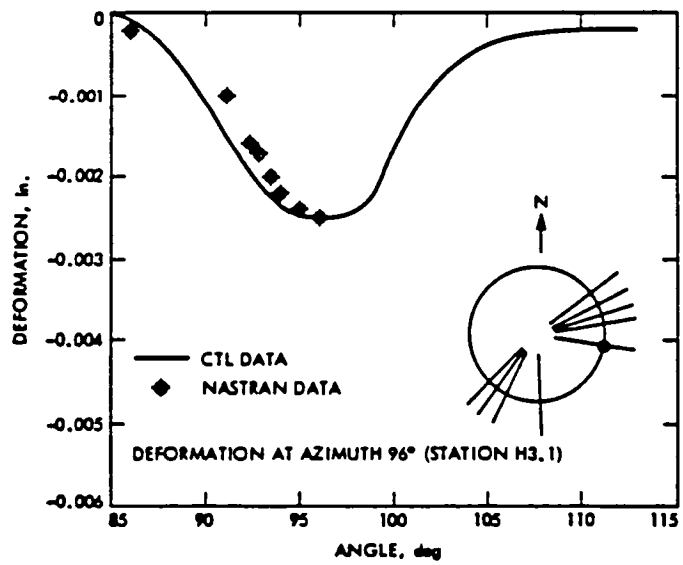

Fig. 16. Comparison of the NASTRAN model results with field test data, azimuth = 96°

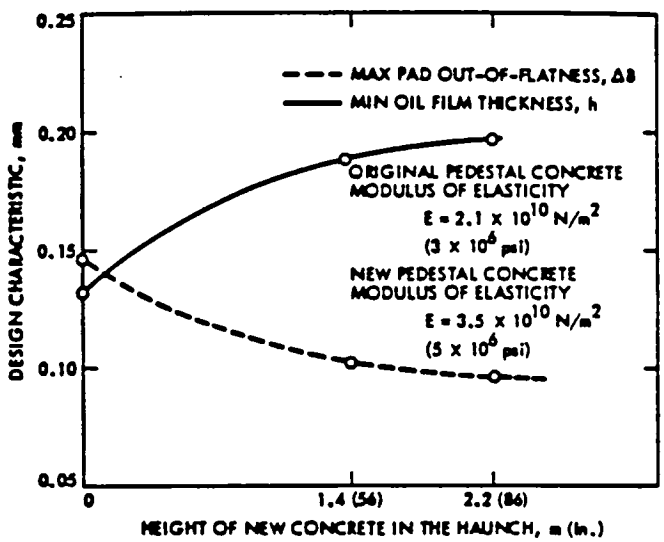

Fig. 17. Effect on the oil film thickness due to the height variation of the new concrete in the pedestal haunch.

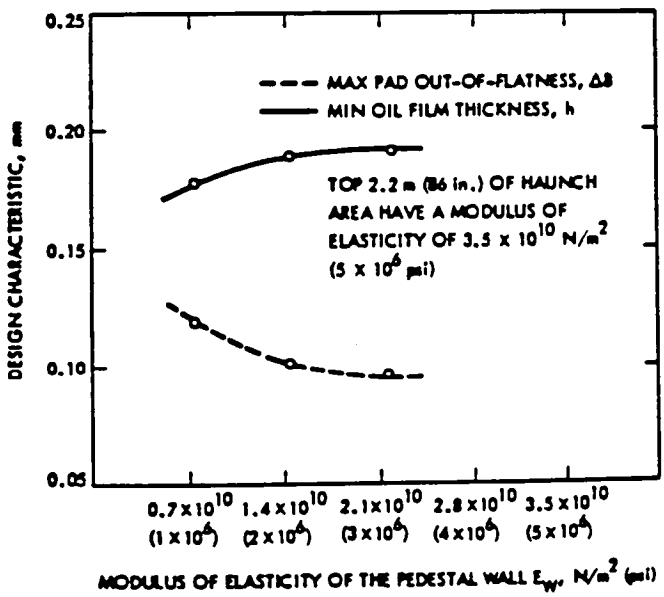

Fig. 18. Effect of varying the modulus of elasticity of the pedestal wall

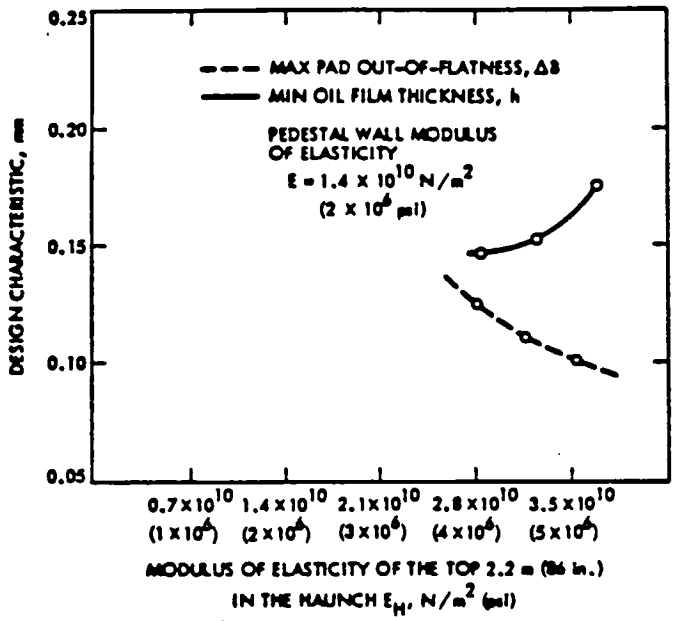

Fig. 19. Effect of varying the modulus of elasticity of the haunch area

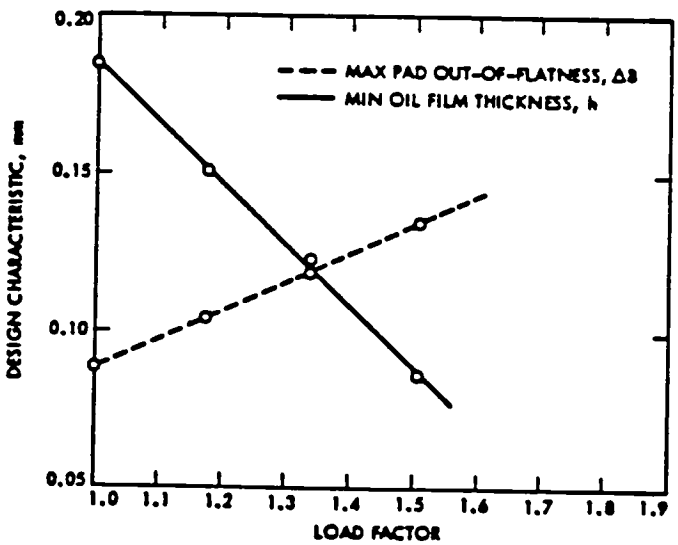

Fig. 20. Effect of the pad load increse due to the antenna extension